Memorias del 2024 Congreso Nacional de Control Automático
8-11 de Octubre, 2024. Ciudad de México, México.

Euler-Lagrange model for balance system of a Testing Bench for Satellite Attitude Determination and Control Systems for 1U CubeSat

A. de J. Pablo-Sotelo * **N. B. Lozada-Castillo** *
A. Luviano-Juárez * **J. J. Hernández-Gómez** **

* *Unidad Profesional Interdisciplinaria en Ingeniería y Tecnologías Avanzadas, Instituto Politécnico Nacional. Av. Luis Enrique Erro S/N, Unidad Profesional Adolfo López Mateos, Zacatenco, Delegación Gustavo A. Madero, 07738, Ciudad de México, México. (e-mail: apablos1800@alumno.ipn.mx).*
** *Centro de Desarrollo Aeroespacial, Instituto Politécnico Nacional Belisario Dominguez 22, Centro, Ciudad de México, 06610, México.*

Abstract: Attitude determination and control systems in nano-satellites require reliable verification systems capable of reproducing the conditions that the system may encounter in space, such as weightlessness, electromagnetic disturbances, etc. In this regard, testing benches commonly use air suspension systems, which require precise initial positioning. For this purpose, mass balance models are employed, allowing the system to reproduce or be controlled under precise and controlled disturbances, closely aligning with the design guidelines set by international space agencies.

Keywords: Modeling, Hardware-in-the-loop simulation, Mechatronic systems, Supervision and testing, Space systems, Attitude Determination and Control Systems.

1. INTRODUCTION

Attitude Determination and Control System (ADCS) are a fundamental part of a satellite mission, as they are responsible for all manoeuvres related to the orientation of the satellite in space. This includes pointing the satellite to a specific location on Earth, conducting interplanetary observations, and orienting the satellite's solar panels toward the sun (Paluszek, 2023; NASA, 2018; Markley and Crassidis, 2014). Due to this, it is necessary to ensure the proper functioning of the ADCS through validation tests, with Hardware-in-the-loop tests being the preferred method. However, having the appropriate infrastructure to perform the necessary tests to validate that the system works correctly is itself a challenge that encompasses three fundamental elements: a Helmholtz cage, a low-friction system, and a disturbance generation system. For the purposes of this work, emphasis will be placed on the low-friction environment generation system. Additionally, we will address the challenges that may arise from setting up the initial conditions for verifying the satellite's ADCS. A balance system for the test plate is proposed as a solution to this issue.

1.1 Low-friction environment

In space, a satellite undergoes multiple physical phenomena, among which microgravity is one that needs to be simulated on the ground to validate the attitude control systems. To this end, multiple solutions are proposed, ranging from using fluids to help maintain the satellite at a constant height above the container in which it is placed, to air bearings, which are by far the most widely used according to the literature (Zhao et al., 2023; El wafi et al., 2024; Gaber et al., 2020; Panyalert et al., 2023). The term "air bearing" refers to the use of pressurised air to generate a thin layer of air between two surfaces, allowing them to move relative to each other without touching. For use in ADCS, spherical air bearings are commonly employed (see Fig. 1), which utilise a concave and a convex smooth surface, allowing rotation with three degrees of freedom (Modenini et al., 2020; Prinkey et al., 2013). The air layer typically has a thickness between 10 and 150 micrometers. This thin layer of air allows the concave and convex surfaces to move relative to each other without contact, creating a low-friction environment and simulating the friction-less environment of space.

Air bearing systems pose a challenge, primarily due to the materials used for the construction of both the plate and the bearing. In this regard, it has been observed that having a balanced system for verification testing is necessary (Kwan et al., 2015; Prinkey et al., 2013; Zhao et al., 2023). Currently, many research centres perform this balancing using unconventional methods, leaving room for unconsidered errors and making characterisation difficult.

⋆ The authors acknowledge partial economical support by projects 20242752, 20240894, 20241163, 20241077 and 20240811, as well as EDI and PIFI grants, provided by Secretaría de Investigación y Posgrado, Instituto Politécnico Nacional.
https://doi.org/10.58571/CNCA.AMCA.2024.017

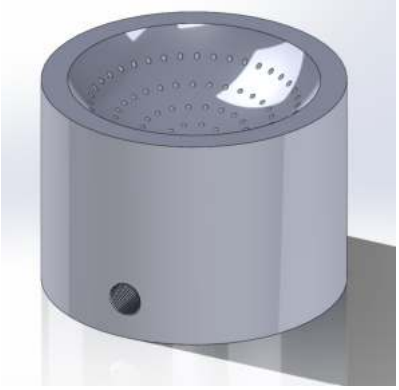

Fig. 1. Tabletop air bearing.

1.2 Test bench design

Multiple test bench designs have been proposed, most of which are characterised by the inclusion of an air bearing, a disturbance generation system, and a Helmholtz cage. For the purposes of this study, Fig. 2 presents a test bench featuring a balancing system with hanging masses on a rigid bar that move across the plane.

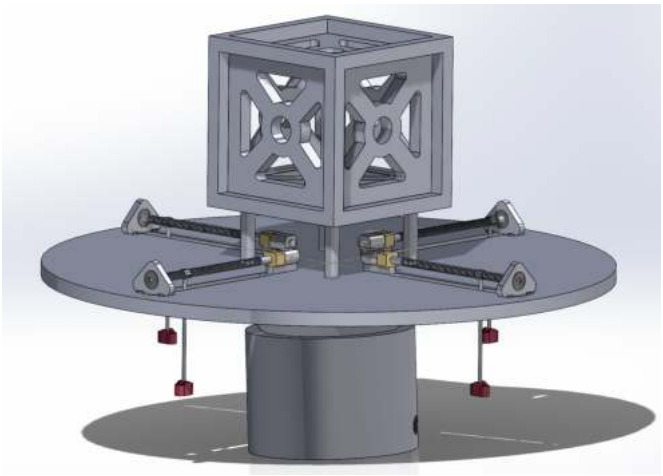

Fig. 2. Test bench.

In the Hardware-in-the-loop (HIL) verification systems discussed in the literature (Shim et al., 2023; Farissi et al., 2019), a recurrent issue is the initial configuration of the system. This problem arises because, although international standards require CubeSat developers to place the geometric centre as close as possible to the satellite's centre of mass (with a deviation of no more than ±2 cm for 1U CubeSat), the challenges of manufacturing and integrating the satellite often result in a centre of mass that, while within the specified limits, causes imbalances. These imbalances lead to unwanted disturbances when the satellite is placed on the test plate for verification testing. This design is characterised by a worm screw mechanism that displaces the masses and balances the system, which is suspended by the air bearing. In order to effectively address the system, a simplified model will be presented for this study (see Fig. 3).

2. EULER-LAGRANGE MODELLING

With the aim of modeling the system using the Euler-Lagrange formulaism, a kinematic analysis is previously

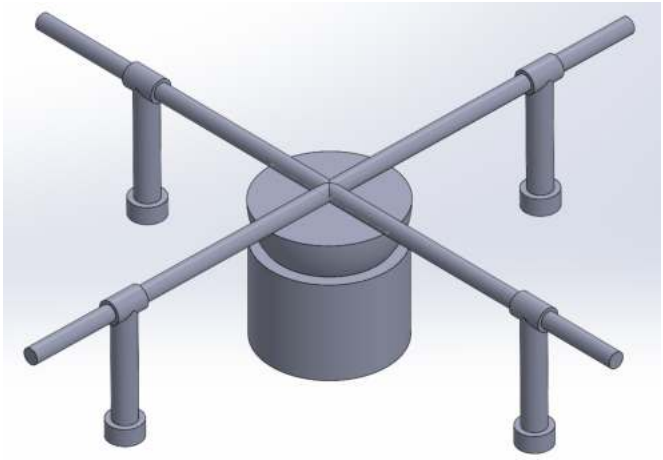

Fig. 3. Simplified model

carried out to find the positions of the masses after certain rotations, always considering the plane. Subsequently, upon finding the positions of the masses based on the two angles of rotation (or inclination), we begin to analyze for the moment the positions of the mass as well as the inclinations of the system.

2.1 Kinematic Analysis

The final position of the model will be determined using transformation matrices; for this, the rotations of the system are determined (see Figure 4 and Fig. 5).

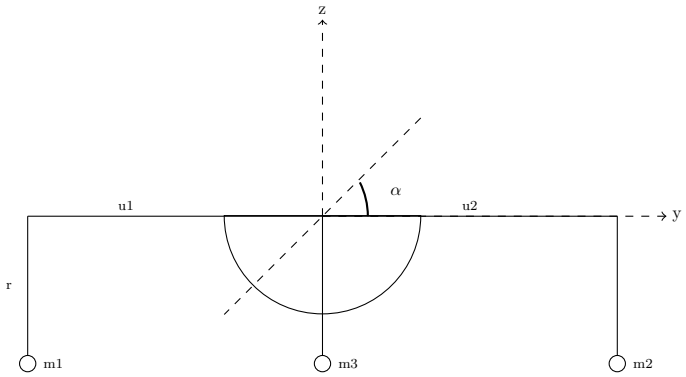

Fig. 4. System's side view.

In Figure 6, the variables U_1, U_2, U_3 and U_4 are the lengths that are determined from the movement of the

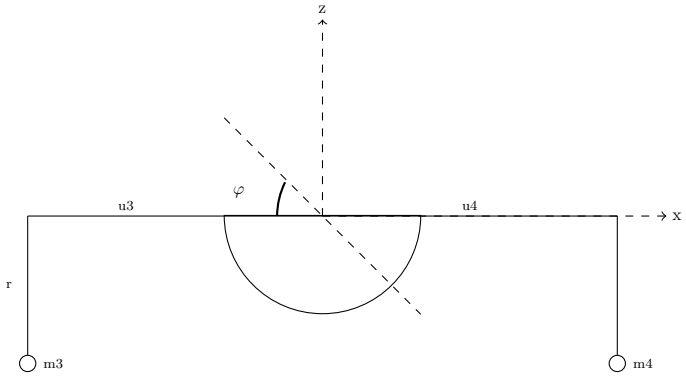

Fig. 5. Second side view of the system.

https://doi.org/10.58571/CNCA.AMCA.2024.017

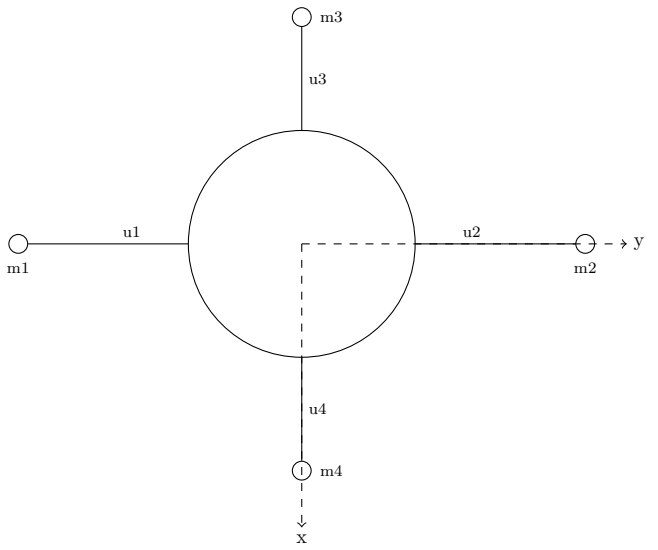

Fig. 6. System's top view

worm screw; on the other hand, the angles α and φ They are the inclinations of the model, in combination. Compiling rotations for the system for a rotation in the X-Y axes. It is worth mentioning that the model considers that the pendulating masses of the system are equal.

$$Rot_{x-y} = Rot_x(\alpha) \cdot Rot_y(\varphi) \tag{1}$$

$$Rot_{x-y} = \begin{bmatrix} 1 & 0 & 0 \\ 0 & C\alpha & -S\alpha \\ 0 & S\alpha & C\alpha \end{bmatrix} \begin{bmatrix} C\varphi & 0 & S\varphi \\ 0 & 1 & 0 \\ -S\varphi & 0 & C\varphi \end{bmatrix} = \begin{bmatrix} C\varphi & 0 & S\varphi \\ S\alpha S\varphi & C\alpha & -S\alpha C\varphi \\ -C\alpha S\varphi & S\alpha & C\alpha C\varphi \end{bmatrix} \tag{2}$$

This rotation will affect each of the positions of the masses, therefore the position of each of the masses is determined according to its initial position with respect to the inertial reference frame. The position of masses one, two, three and four are described below where the subscript indicates the mass referenced in the inertial reference frame located at the centre of the air bearing.

$$\begin{bmatrix} x_1 \\ y_1 \\ z_1 \end{bmatrix} = \begin{bmatrix} C\varphi & 0 & S\varphi \\ S\alpha S\varphi & C\alpha & -S\alpha C\varphi \\ -C\alpha S\varphi & S\alpha & C\alpha C\varphi \end{bmatrix} \begin{bmatrix} x_{1_i} \\ y_{1_i} \\ z_{1_i} \end{bmatrix} = \begin{bmatrix} -rS\varphi \\ -u_1 C\alpha + rS\alpha C\varphi \\ -u_1 S\alpha - rC\alpha C\varphi \end{bmatrix} \tag{3}$$

$$\begin{bmatrix} x_2 \\ y_2 \\ z_2 \end{bmatrix} = \begin{bmatrix} C\varphi & 0 & S\varphi \\ S\alpha S\varphi & C\alpha & -S\alpha C\varphi \\ -C\alpha S\varphi & S\alpha & C\alpha C\varphi \end{bmatrix} \begin{bmatrix} x_{2_i} \\ y_{2_i} \\ z_{2_i} \end{bmatrix} = \begin{bmatrix} -rS\varphi \\ -u_2 C\alpha + S\alpha C\varphi \\ u_2 S\alpha - rC\alpha C\varphi \end{bmatrix} \tag{4}$$

$$\begin{bmatrix} x_3 \\ y_3 \\ z_3 \end{bmatrix} = \begin{bmatrix} C\varphi & 0 & S\varphi \\ S\alpha S\varphi & C\alpha & -S\alpha C\varphi \\ -C\alpha S\varphi & S\alpha & C\alpha C\varphi \end{bmatrix} \begin{bmatrix} x_{3_i} \\ y_{3_i} \\ z_{3_i} \end{bmatrix} = \begin{bmatrix} -u_3 C\varphi + rS\varphi \\ -u_3 S\alpha S\varphi - rS\alpha C\varphi \\ u_3 C\alpha S\varphi + rC\alpha C\varphi \end{bmatrix} \tag{5}$$

$$\begin{bmatrix} x_4 \\ y_4 \\ z_4 \end{bmatrix} = \begin{bmatrix} C\varphi & 0 & S\varphi \\ S\alpha S\varphi & C\alpha & -S\alpha C\varphi \\ -C\alpha S\varphi & S\alpha & C\alpha C\varphi \end{bmatrix} \begin{bmatrix} x_{4_i} \\ y_{4_i} \\ z_{4_i} \end{bmatrix} = \begin{bmatrix} u_4 C\varphi + rS\varphi \\ u_4 S\alpha S\varphi - rS\alpha C\varphi \\ -u_4 C\alpha S\varphi + rC\alpha C\varphi \end{bmatrix} \tag{6}$$

2.2 Euler-Lagrange model

From the positions found in the Equation (3), (4), (5) and (6) the norm 2 of the squared velocity is found by performing the corresponding derivatives

$$\begin{aligned} ||\boldsymbol{v_1}||_2^2 = {} & r^2\varphi'^2\cos^2(\varphi) + \big(r\left(\alpha'\cos(\alpha)\cos(\varphi) - \right. \\ & \left.\sin(\alpha)\varphi'\cos(\varphi)\right) - \cos(\alpha){U_1}' + \\ & U_1\alpha'\sin(\alpha)\big)^2 + \big(-r\left(\alpha'\sin(\alpha)(-\cos(\varphi)) - \right. \\ & \left.\cos(\alpha)\varphi'\sin(\varphi)\right) - \sin(\alpha){U_1}' - U_1\alpha'\cos(\alpha)\big)^2 \end{aligned} \tag{7a}$$

$$\begin{aligned} ||\boldsymbol{v_2}||_2^2 = {} & r^2\varphi'^2\cos^2(\varphi) + \big(r\left(\alpha'\cos(\alpha)\cos(\varphi) - \right. \\ & \left.\sin(\alpha)\varphi'\cos(\varphi)\right) + \cos(\alpha){U_2}' - \\ & U_2\alpha'\sin(\alpha)\big)^2 + \big(-r\left(\alpha'\sin(\alpha)(-\cos(\varphi)) - \right. \\ & \left.\cos(\alpha)\varphi'\sin(\varphi)\right) + \sin(\alpha){U_2}' + U_2\alpha'\cos(\alpha)\big)^2 \end{aligned} \tag{7b}$$

$$\begin{aligned} ||\boldsymbol{v_3}||_2^2 = {} & \big(-r\alpha'\sin(\alpha)\cos(\varphi) - \\ & r\cos(\alpha)\varphi'\sin(\varphi) + \cos(\alpha){U_3}'\sin(\varphi) - \\ & U_3\alpha'\sin(\alpha)\sin(\varphi) + U_3\cos(\alpha)\varphi'\cos(\varphi)\big)^2 + \\ & \big(-r\alpha'\cos(\alpha)\cos(\varphi) + r\sin(\alpha)\varphi'\sin(\varphi) - \\ & \sin(\alpha){U_3}'\sin(\varphi) - U_3\alpha'\cos(\alpha)\sin(\varphi) - \\ & U_3\sin(\alpha)\varphi'\cos(\varphi)\big)^2 + \big(r\varphi'\cos(\varphi) + \\ & {U_3}'(-\cos(\varphi)) + U_3\varphi'\sin(\varphi)\big)^2 \end{aligned} \tag{7c}$$

$$\begin{aligned} ||\boldsymbol{v_4}||_2^2 = {} & \big(-r\alpha'\cos(\alpha)\cos(\varphi) + \\ & r\sin(\alpha)\varphi'\sin(\varphi) + \sin(\alpha){U_4}'\sin(\varphi) + \\ & U_4\alpha'\cos(\alpha)\sin(\varphi) + U_4\sin(\alpha)\varphi'\cos(\varphi)\big)^2 + \\ & \big(-r\alpha'\sin(\alpha)\cos(\varphi) - r\cos(\alpha)\varphi'\sin(\varphi) - \\ & \cos(\alpha){U_4}'\sin(\varphi) + U_4\alpha'\sin(\alpha)\sin(\varphi) - \\ & U_4\cos(\alpha)\varphi'\cos(\varphi)\big)^2 + \big(r\varphi'\cos(\varphi) + \\ & {U_4}'\cos(\varphi) - U_4\varphi'\sin(\varphi)\big)^2 \end{aligned} \tag{7d}$$

We now start to find the kinetic energy of the system which is described by the Equation 8

$$\begin{aligned} T = {} & \frac{1}{2}m\Big(r^2\varphi'^2\cos^2(\varphi) + \big(r\left(\alpha'\cos(\alpha)\cos(\varphi) - \right. \\ & \left.\sin(\alpha)\varphi'\cos(\varphi)\right) - \cos(\alpha){U_1}' + U_1\alpha'\sin(\alpha)\big)^2 + \\ & \big(-r\left(\alpha'\sin(\alpha)(-\cos(\varphi)) - \cos(\alpha)\varphi'\sin(\varphi)\right) - \\ & \sin(\alpha){U_1}' - U_1\alpha'\cos(\alpha)\big)^2\Big) + \frac{1}{2}m\Big(r^2\varphi'^2\cos^2(\varphi) + \\ & \big(r\left(\alpha'\cos(\alpha)\cos(\varphi) - \sin(\alpha)\varphi'\cos(\varphi)\right) + \cos(\alpha){U_2}' - \\ & U_2\alpha'\sin(\alpha)\big)^2 + \big(-r\left(\alpha'\sin(\alpha)(-\cos(\varphi)) - \right. \\ & \left.\cos(\alpha)\varphi'\sin(\varphi)\right) + \sin(\alpha){U_2}' + U_2\alpha'\cos(\alpha)\big)^2\Big) + \\ & \frac{1}{2}m\Big(\big(-r\alpha'\sin(\alpha)\cos(\varphi) - r\cos(\alpha)\varphi'\sin(\varphi) + \\ & \cos(\alpha){U_3}'\sin(\varphi) - U_3\alpha'\sin(\alpha)\sin(\varphi) + \\ & U_3\cos(\alpha)\varphi'\cos(\varphi)\big)^2 + \big(-r\alpha'\cos(\alpha)\cos(\varphi) + \\ & r\sin(\alpha)\varphi'\sin(\varphi) - \sin(\alpha){U_3}'\sin(\varphi) - \\ & U_3\alpha'\cos(\alpha)\sin(\varphi) - U_3\sin(\alpha)\varphi'\cos(\varphi)\big)^2 + \\ & \big(r\varphi'\cos(\varphi) + {U_3}'(-\cos(\varphi)) + U_3\varphi'\sin(\varphi)\big)^2\Big) + \\ & \frac{1}{2}m\Big(\big(-r\alpha'\cos(\alpha)\cos(\varphi) + r\sin(\alpha)\varphi'\sin(\varphi) + \\ & \sin(\alpha){U_4}' + U_4\alpha'\cos(\alpha)\sin(\varphi) + \\ & U_4\sin(\alpha)\varphi'\cos(\varphi)\big)^2 + \big(-r\alpha'\sin(\alpha)\cos(\varphi) - \\ & r\cos(\alpha)\varphi'\sin(\varphi) - \cos(\alpha){U_4}'\sin(\varphi) + \\ & U_4\alpha'\sin(\alpha)\sin(\varphi) - U_4\cos(\alpha)\varphi'\cos(\varphi)\big)^2 + \\ & \big(r\varphi'\cos(\varphi) + {U_4}'\cos(\varphi) - U_4\varphi'\sin(\varphi)\big)^2\Big) \end{aligned} \tag{8}$$

https://doi.org/10.58571/CNCA.AMCA.2024.017

On the other hand, the potential energy (See Equation 9) of the system is determined by the position of the masses in their respective axes in Z (See Equation 3, 4, 5 and 6)

$$\begin{aligned} V = &-gm(-r\cos(\alpha)\cos(\varphi) - U_1\sin(\alpha)) - \\ &gm(U_2\sin(\alpha) - r\cos(\alpha)\cos(\varphi)) - \\ &gm(r\cos(\alpha)\cos(\varphi) + U_3\cos(\alpha)\sin(\varphi)) - \\ &gm(r\cos(\alpha)\cos(\varphi) - U_4\cos(\alpha)\sin(\varphi)) \end{aligned} \tag{9}$$

The Lagrangian of the system is then constructed

$$\begin{aligned} \mathcal{L} = &gm(-r\cos(\alpha)\cos(\varphi) - U_1\sin(\alpha)) + gm(U_2\sin(\alpha) - \\ &r\cos(\alpha)\cos(\varphi)) + gm(r\cos(\alpha)\cos(\varphi) + \\ &U_3\cos(\alpha)\sin(\varphi)) + gm(r\cos(\alpha)\cos(\varphi) - \\ &U_4\cos(\alpha)\sin(\varphi)) + \frac{1}{2}m\left(r^2\varphi'^2\cos^2(\varphi) + \right. \\ &\left(r\left(\alpha'\cos(\alpha)\cos(\varphi) - \sin(\alpha)\varphi'\cos(\varphi)\right) - \right. \\ &\left.\cos(\alpha){U_1}' + U_1\alpha'\sin(\alpha)\right)^2 + \left(-r\left(\alpha'\sin(\alpha)(-\right.\right. \\ &\left.\cos(\varphi)) - \cos(\alpha)\varphi'\sin(\varphi)\right) - \sin(\alpha){U_1}' - \\ &\left.U_1\alpha'\cos(\alpha)\right)^2\Big) + \frac{1}{2}m\left(r^2\varphi'^2\cos^2(\varphi) + \right. \\ &\left(r\left(\alpha'\cos(\alpha)\cos(\varphi) - \sin(\alpha)\varphi'\cos(\varphi)\right) + \cos(\alpha){U_2}' - \right. \\ &\left.U_2\alpha'\sin(\alpha)\right)^2 + \left(-r\left(\alpha'\sin(\alpha)(-\cos(\varphi)) - \right.\right. \\ &\left.\left.\cos(\alpha)\varphi'\sin(\varphi)\right) + \sin(\alpha){U_2}' + U_2\alpha'\cos(\alpha)\right)^2\Big) + \\ &\frac{1}{2}m\left(\left(-r\alpha'\sin(\alpha)\cos(\varphi) - r\cos(\alpha)\varphi'\sin(\varphi) + \right.\right. \\ &\left.\cos(\alpha){U_3}'\sin(\varphi) - U_3\alpha'\sin(\alpha)\sin(\varphi) + \right. \\ &\left.U_3\cos(\alpha)\varphi'\cos(\varphi)\right)^2 + \left(-r\alpha'\cos(\alpha)\cos(\varphi) + \right. \\ &\left.r\sin(\alpha)\varphi'\sin(\varphi) - \sin(\alpha){U_3}'\sin(\varphi) - \right. \\ &\left.U_3\alpha'\cos(\alpha)\sin(\varphi) - U_3\sin(\alpha)\varphi'\cos(\varphi)\right)^2 + \\ &\left.\left(r\varphi'\cos(\varphi) + {U_3}'(-\cos(\varphi)) + U_3\varphi'\sin(\varphi)\right)^2\right) + \\ &\frac{1}{2}m\left(\left(-r\alpha'\cos(\alpha)\cos(\varphi) + r\sin(\alpha)\varphi'\sin(\varphi) + \right.\right. \\ &\left.\sin(\alpha){U_4}'\sin(\varphi) + U_4\alpha'\cos(\alpha)\sin(\varphi) + \right. \\ &\left.U_4\sin(\alpha)\varphi'\cos(\varphi)\right)^2 + \left(-r\alpha'\sin(\alpha)\cos(\varphi) - \right. \\ &\left.r\cos(\alpha)\varphi'\sin(\varphi) - \cos(\alpha){U_4}'\sin(\varphi) + \right. \\ &\left.U_4\alpha'\sin(\alpha)\sin(\varphi) - U_4\cos(\alpha)\varphi'\cos(\varphi)\right)^2 + \\ &\left.\left(r\varphi'\cos(\varphi) + {U_4}'\cos(\varphi) - U_4\varphi'\sin(\varphi)\right)^2\right) \end{aligned} \tag{10}$$

Remembering the structure of the Euler-Lagrange expression

$$\frac{d}{dt}\frac{\partial\mathcal{L}(q)}{\partial\dot{q}} - \frac{\partial\mathcal{L}(q)}{\partial q} = 0 \tag{11}$$

For each of the generalised coordinates ($\alpha, \varphi, U_1, U_2, U_3$ and U_4) the system is then described by the Equations 12, 13, 14, 15, 16 and 17.

$$\begin{aligned} &\frac{1}{2}m\left(2\sin(\varphi)\left(gU_3\sin(\alpha) - gU_4\sin(\alpha) + \right.\right. \\ &r\cos^2(\alpha)\varphi'\left({U_1}' - {U_2}'\right) + \\ &\left.r(U_1 - U_2)\left(\sin^2(\alpha)\varphi'^2 - \cos^2(\alpha)\varphi''\right)\right) + \\ &2gU_1\cos(\alpha) - 2gU_2\cos(\alpha) + 4r^2\alpha'' - r^2\sin(2\alpha)\varphi'' + \\ &\sin(2\varphi)\left(r^2\sin(2\alpha)\left(\varphi'' + 2\varphi'^2\right) + \right. \\ &2\alpha'\left(\varphi'\left(-4r^2 + {U_3}^2 + {U_4}^2\right) + r{U_3}' - r{U_4}'\right) + \\ &\left.2r\alpha''(U_3 - U_4)\right) - \cos(2\varphi)\left(r^2\left(\sin(2\alpha)\varphi'' - 4\alpha''\right) + \right. \\ &2U_3\alpha'\left({U_3}' - 2r\varphi'\right) + 2U_4\alpha'\left(2r\varphi' + {U_4}'\right) + {U_3}^2\alpha'' + \\ &\left.{U_4}^2\alpha''\right) + 2r\cos(\varphi)\left(-{U_1}'' + \cos^2(\alpha)\varphi'\left(-{U_1}' + \right.\right. \\ &\left.\left.(U_2 - U_1)\varphi' + {U_2}'\right) + \sin^2(\alpha)(U_2 - U_1)\varphi'' + {U_2}''\right) + \\ &4U_1\alpha'{U_1}' + 2{U_1}^2\alpha'' + 4U_2\alpha'{U_2}' + 2{U_2}^2\alpha'' + \\ &\left.2U_3\alpha'{U_3}' + {U_3}^2\alpha'' + 2U_4\alpha'{U_4}' + {U_4}^2\alpha''\right) = 0 \end{aligned} \tag{12}$$

$$\begin{aligned} &\frac{1}{2}m\left(\cos(\varphi)\left(2g\cos(\alpha)(U_4 - U_3) + \right.\right. \\ &r\left(\sin(2\alpha)\left({U_1}'' + 2\alpha'^2(U_2 - U_1) - {U_2}''\right) + \right. \\ &\alpha'(3\cos(2\alpha) - 1){U_1}' + 2\alpha''\sin^2(\alpha)(U_2 - U_1) + \\ &\left.\alpha'(1 - 3\cos(2\alpha)){U_2}'\right)\Big) - r^2\alpha''\sin(2\alpha) - 2r^2\alpha'^2\cos(2\alpha) + \\ &\sin(2\varphi)\left(2r^2\sin(\alpha)\left(\alpha''\cos(\alpha) - 2\sin(\alpha)\varphi'^2\right) + \right. \\ &\left.\alpha'^2\left(2r^2(\cos(2\alpha) + 2) - {U_3}^2 - {U_4}^2\right)\right) + 8r^2\varphi'' + \\ &2r\cos(\alpha)\sin(\varphi)\left(\sin(\alpha)\left(-{U_1}'' + 2\alpha'^2(U_1 - U_2) + \right.\right. \\ &\left.\left.{U_2}''\right) + \cos(\alpha)\left(3\alpha'\left({U_2}' - {U_1}'\right) + \alpha''(U_2 - U_1)\right)\right) \\ &- 2r{U_3}'' - r\cos(2\varphi)\left(2r\sin(\alpha)\left(\alpha''\cos(\alpha) - 2\sin(\alpha)\varphi''\right)\right. \\ &\left.- 4r\alpha'\sin(2\alpha)\varphi' + 2\alpha'^2(r\cos(2\alpha) + U_3 - U_4)\right) + \\ &\left.2r{U_4}'' + 4U_3{U_3}'\varphi' + 2{U_3}^2\varphi'' + 4U_4{U_4}'\varphi' + 2{U_4}^2\varphi''\right) = 0 \end{aligned} \tag{13}$$

$$\begin{aligned} &m\left(g\sin(\alpha) + \frac{1}{2}r\left(-2\alpha''\cos(\varphi) + \right.\right. \\ &\alpha'\varphi'\left(2\cos^2(\alpha)\cos(\varphi) - (\cos(2\alpha) - 3)\sin(\varphi)\right) + \\ &\sin(2\alpha)\left(\varphi''(\cos(\varphi) - \sin(\varphi)) - \varphi'^2(\sin(\varphi) + \right. \\ &\left.\left.\left.\cos(\varphi))\right)\right) + {U_1}'' - U_1\alpha'^2\Big) = 0 \end{aligned} \tag{14}$$

$$\begin{aligned} &m\left(-g\sin(\alpha) + \frac{1}{2}r\left(2\alpha''\cos(\varphi) + \right.\right. \\ &\alpha'\varphi'\left(\left(\cos(2\alpha) - 3\right)\sin(\varphi) - 2\cos^2(\alpha)\cos(\varphi)\right) + \\ &\sin(2\alpha)\left(\varphi''(\sin(\varphi) - \cos(\varphi)) + \right. \\ &\left.\left.\left.\varphi'^2(\sin(\varphi) + \cos(\varphi))\right)\right) + {U_2}'' - U_2\alpha'^2\Big) = 0 \end{aligned} \tag{15}$$

$$\begin{aligned} &-m\left(g\cos(\alpha)\sin(\varphi) + \alpha'^2\sin(\varphi)(r\cos(\varphi) + \right. \\ &\left.U_3\sin(\varphi)) + r\varphi'' - {U_3}'' + U_3\varphi'^2\right) = 0 \end{aligned} \tag{16}$$

https://doi.org/10.58571/CNCA.AMCA.2024.017

$$
\begin{aligned}
& m\left(g\cos(\alpha)\sin(\varphi)+\right. \\
& \quad \alpha'^{2}\sin(\varphi)(r\cos(\varphi)-U_4\sin(\varphi))+ \\
& \quad \left. r\varphi''+U_4''-U_4\varphi'^{2}\right)=0
\end{aligned} \tag{17}
$$

3. CONCLUSIONS

In this study, we have successfully developed a comprehensive model for a balancing system designed for 1U CubeSat HIL testing of ADCS. Our approach employed a rigorous kinematic description using rotation matrices, which served as the basis for the subsequent Euler-Lagrange formulation. The resulting six equations predominantly contain angular elements, highlighting the system's complex, nonlinear dynamics. This insight is vital for understanding the balancing system's behaviour under various conditions. Looking forward, we propose three key areas for future work: first, linearising the system could significantly enhance its analysis and potentially lead to simplified control strategies; second, the development of an active control system for balancing the CubeSat remains an important research direction; and third, an alternative modelling approach focusing on locating and tracking the system's centre of mass could provide additional insights. As the space industry continues to evolve, particularly in the realm of small satellites, such detailed modelling approaches will play a crucial role in advancing our capabilities in satellite design and testing.

REFERENCES

El wafi, I., Haloua, M., Guennoun, Z., and Moudden, Z. (2024). A framework for developing an attitude determination and control system simulator for cubesats: Processor-in-loop testing approach. *Results in Engineering*, 22. doi:10.1016/j.rineng.2024.102201. Cited by: 0; All Open Access, Gold Open Access.

Farissi, M.S., Carletta, S., and Nascetti, A. (2019). Design and hardware-in-the-loop test of an active magnetic detumbling and pointing control based only on three-axis magnetometer data. volume 2019-October. Cited by: 2.

Gaber, K., ElMashade, M., and Aziz, G.A.A. (2020). Hardware-in-the-loop real-time validation of microsatellite attitude control. *Comput. Electr. Eng.*, 85, 106679. doi:10.1016/j.compeleceng.2020.106679.

Kwan, T., Lee, K.M.B., Yan, J., and Wu, X. (2015). An air bearing table for satellite attitude control simulation. 1420–1425. doi:10.1109/ICIEA.2015.7334330.

Markley, F.L. and Crassidis, J.L. (2014). *Fundamentals of Spacecraft Attitude Determination and Control*. Springer, New York, Heidelberg, Dordrecht, London. doi:10.1007/978-1-4939-0802-8.

Modenini, D., Bahu, A., Curzi, G., and Togni, A. (2020). A dynamic testbed for nanosatellites attitude verification. *Aerospace*, 7(3). doi:10.3390/aerospace7030031. Cited by: 22; All Open Access, Gold Open Access.

NASA (2018). *State of the Art Small Spacecraft Technology*. National Aeronautics and Space Administration, Ames Research Center, Moffett Field, California. NASA/TP–2018-220027.

Paluszek, M. (2023). *ADCS - Spacecraft Attitude Determination and Control*. Elsevier. doi:https://doi.org/10.1016/B978-0-32-399915-1.00038-3.

Panyalert, T., Manuthasna, S., Chaisakulsurin, J., Masri, T., Palee, K., Prasit, P., Torteeka, P., Poonpakdee, P., and Konghuayrob, P. (2023). Experimental verification of control strategies for satellite magnetic-based attitude control system under a three-axis helmholtz cage environment. 771 – 776. doi:10.1109/TENCON58879.2023.10322440. Cited by: 0.

Prinkey, M.K., Miller, D.W., Bauer, P., Cahoy, K., Wise, E.D., Pong, C.M., Kingsbury, R.W., Marinan, A.D., Lee, H.W., and Main, E.L. (2013). Cubesat attitude control testbed design: Merritt 4-coil per axis helmholtz cage and spherical air bearing. Cited by: 9.

Shim, H., Kim, O.J., Park, M., Choi, M., and Kee, C. (2023). Development of hardware-in-the-loop simulation for cubesat platform: Focusing on magnetometer and magnetorquer. *IEEE Access*, 11, 73164 – 73179. doi:10.1109/ACCESS.2023.3294565. Cited by: 0; All Open Access, Gold Open Access.

Zhao, Z., Sun, L., Qiao, Y., Duan, S., Zhang, T., and Amir (2023). Design and development of an adcs teaching platform for educational small satellite. volume 2023-October. Cited by: 0.

